10.1098/rsta.2003.1360

THE ROYAL SOCIETY

Designing for chaos: applications of chaotic advection at the microscale

By Mark A. Stremler[1], F. R. Haselton[2] and Hassan Aref[3]

[1]*Department of Mechanical Engineering, Vanderbilt University, VU Station B 351592, 2301 Vanderbilt Place, Nashville, TN 37235-1592, USA* (mark.stremler@vanderbilt.edu)

[2]*Department of Biomedical Engineering, Vanderbilt University, VU Station B 351631, 2301 Vanderbilt Place, Nashville, TN 37235-1631, USA*

[3]*College of Engineering, Virginia Polytechnic Institute and State University, 333 Norris Hall, Blacksburg, VA 24061-0217, USA*

Published online 11 March 2004

Chaotic advection can play an important role in efficient microfluidic mixers. We discuss a design paradigm that exploits chaotic advection and illustrate by two recent examples, namely enhancing gene expression profiling and constructing an in-line microfluidic mixing channel, how application of this paradigm has led to successful micromixers. We suggest that 'designing for chaos', that is, basing practical mixer design on chaotic advection analysis, is a promising approach to adopt in this developing field which otherwise has little to guide it and is constrained by issues of scale and manufacturability.

Keywords: micro-electrical mechanical systems (MEMS); chaos; chaotic advection; microfluidics; mixing

1. Introduction

Over the past decade, microfluidics has emerged as an important subject for research in fluid mechanics. Early interest in microelectronics cooling (Tuckerman & Pease 1981) has expanded into a comprehensive study of transport and mixing in microfluidic systems, including applications to chemical and biological analysis. Numerous reviews of these applications have appeared in the literature over the past few years (Cunningham 2001; Kakuta *et al*. 2001; Beebe *et al*. 2002; Chován & Guttman 2002; Meldrum & Holl 2002; Schulte *et al*. 2002; Sato *et al*. 2003; Weigl *et al*. 2003), and several earlier reviews are also available. Reviews and monographs that focus specifically on the development of microfluidics have also appeared recently (Stone & Kim 2001; Whitesides & Stroock 2001; Gad-el-Hak 2002; Nguyen & Wereley 2002).

Each of the reviews above highlights the importance of fluid mixing to one or more target applications. A common theme is that the size of microfluidic devices

One contribution of 11 to a Theme 'Transport and mixing at the microscale'.

Table 1. *Microfluidic mixers in the literature*

(Semicolon-delimited citations indicate related investigations performed by members of the same group.)

passive mixers	
laminar jets	Miyake *et al.* (1993), Böhm *et al.* (2001)
meniscus recirculation	Evensen *et al.* (1998), Anderson *et al.* (1998), Song *et al.* (2003)
parallel lamination	Koch *et al.* (1998), Erbacher *et al.* (1999) Ehrfeld *et al.* (1999); Haverkamp *et al.* (1999) Bessoth *et al.* (1999); Mitchell *et al.* (2000); Xu *et al.* (2000) He *et al.* (2001)
serial lamination with fluid dynamics	Branebjerg *et al.* (1994) Liu *et al.* (2000); Beebe *et al.* (2001); Vijayendran *et al.* (2003) Stroock *et al.* (2002), Therriault *et al.* (2003)
serial lamination with physical splitting	Mensinger *et al.* (1994), Schwesinger *et al.* (1996), Branebjerg *et al.* (1996), Gray *et al.* (1999), Bertsch *et al.* (2001), Hong *et al.* (2001), Wang *et al.* (2002)
junctions and hydrodynamic focusing	Bökenkamp *et al.* (1999) Knight *et al.* (1998); Pollack *et al.* (1999) Greiner *et al.* (2000), Gobby *et al.* (2001), Pabit & Hagen (2002), Anna *et al.* (2003)
active mixers	
acoustic vibration	Moroney *et al.* (1991), Woias *et al.* (2000) Zhu & Kim (1998); Vivek *et al.* (2000) Rife *et al.* (2000), Yasuda (2000) Yang *et al.* (2000, 2001), Liu *et al.* (2002, 2003) Jagannathan *et al.* (2003)
electrokinetic	Choi *et al.* (2001), Oddy *et al.* (2001) Ajdari (2001), Lee *et al.* (2001)
magnetohydrodynamic	Bau *et al.* (2001)
meniscus recirculation with time dependence	Evensen *et al.* (1998) Hosokawa *et al.* (2000)
pulsed junctions	Volpert *et al.* (1999), Deshmukh *et al.* (2000) Lee *et al.* (2001); Niu & Lee (2003) Glasgow & Aubry (2003)
pulsed lamination	Hinsmann *et al.* (2001)
pulsed chamber	Evans *et al.* (1997), Adey *et al.* (2002), McQuain *et al.* (2004)
stirring	Lu *et al.* (2001), Yuen *et al.* (2003)

makes mixing difficult. Despite the small length-scales involved, with the characteristic dimension typically of the order of 10–100 μm, mixing solely by molecular diffusion is too slow for many applications. Augmenting diffusion is of particular importance in flows containing large biomolecules, for which diffusion is over two orders of magnitude slower than thermal diffusion. Reynolds numbers in flows at this scale generally vary from less than unity up to a few hundred, well within the range of laminar flow (Sharp *et al*. 2002), so the efficient mixing obtained with turbulence is, in most cases, not practically attainable. Furthermore, fabrication constraints often limit the use of standard macroscale mixing techniques such as mechanical stirring. Specific focus has thus been given to developing devices that mix fluids effectively and are practical for implementation on the microscale. Table 1 lists a number of the designs that have been presented in the literature.

Mixing in laminar flows can be enhanced through *chaotic advection*, the phenomenon in which passive particles advected by a periodic velocity field exhibit chaotic trajectories (Aref 1984, 1990, 2002; Ottino 1989). Relative to integrable advection, chaotic advection enhances stretching and folding of material interfaces. This deformation of fluid–fluid boundaries increases the interfacial area across which diffusion occurs, which typically leads to significantly more rapid mixing.

Chaotic motion of fluid particles in laminar flow was first demonstrated in the 1960s with two related studies of the so-called ABC (Arnold–Beltrami–Childress) flow, a class of rather special flows in which the vorticity vector is everywhere parallel to the velocity vector (Arnol'd 1965; Hénon 1966). However, the concept of chaotic advection did not take root in the fluid mechanics community until the investigation of transport in the potential flow of two point vortices alternately 'blinked' on and off (Aref 1984) and the understanding that chaotic advection is, in fact, the general expectation in two-dimensional (2D), unsteady flow (see, for example, Aref 2002). At a minimum, chaotic advection requires unsteady two-dimensional flow or steady three-dimensional flow of a certain complexity.

Since the mid 1980s, a substantial number of investigators have demonstrated that chaotic advection can occur in a wide variety of laminar flows, from creeping flow to potential flow, and in a number of different flow systems, including unsteady two-dimensional flow and both steady and time-periodic three-dimensional flow. Overviews of the early work in the field can be found in Ottino (1989) and Aref (1990). Here we note, in particular, the investigations of eccentric journal bearing flow (Aref & Balachandar 1986; Chaiken *et al*. 1986, 1987), lid-driven cavity flow (Chien *et al*. 1986; Leong & Ottino 1989), pulsed source–sink flow (Jones & Aref 1988), and twisted-pipe flow (Jones *et al*. 1989). More recently, chaotic advection has been observed and studied in numerous additional systems, including various Taylor–Couette flows (Ashwin & King 1995; Mezić 2001), two-dimensional (Rom-Kedar & Poje 1999; Krasny & Nitsche 2002; Boyland *et al*. 2003) and three-dimensional (MacKay 1994; Solomon & Mezić 2003) time-periodic vortex flows, two-dimensional cellular flow (Rothstein *et al*. 1999), open cavity flow (Horner *et al*. 2002), and stirred tanks (Meleshko & Aref 1996; Boyland *et al*. 2000; Finn *et al*. 2003). Applications of mixing by chaotic advection have included heat-transfer enhancement (Ghosh *et al*. 1992; Bryden & Brenner 1996; Ganesan *et al*. 1997; Mokrani *et al*. 1997) and novel polymer processing (see, for example, Zumbrunnen & Inamdar 2001; Kwon & Zumbrunnen 2001).

The demonstrated ability of chaotic advection to enhance mixing in laminar flows on the macroscale and the fact that chaotic advection occurs in numerous geometries and under a variety of flow conditions makes it an obvious tool for designing devices that mix well on the microscale. The term 'designing for chaos' was suggested by R. J. Adrian during the work reported in Liu *et al.* (2000). This approach presents the following paradigm for achieving efficient mixing on the microscale. Firstly, the needs of the intended application are matched to a flow system known to generate chaotic advection, giving a general device configuration. A specific mixer is then designed that meets the application requirements and the fabrication constraints. The resulting device is modelled, and diagnostics are computed to verify the occurrence of chaotic advection. Iterations can then be made on the design to optimize the extent and characteristics of the chaos. Finally, the device is tested experimentally to verify that mixing is indeed enhanced.

In §§ 2 and 3, we discuss the application of 'designing for chaos' to two microfluidic systems: active mixing of a fixed fluid volume in a pulsed source–sink chamber and passive mixing in a flow-through microchannel.

2. Active mixing in a pulsed source–sink chamber

Massively parallel expression screening is an important biological tool that is used widely in genomic research (DeRisi & Iyer 1999; Heller 2002; Mohr *et al.* 2002; Bertucci *et al.* 2003). This technology, known primarily as *microarray analysis*, uses a surface spotted with immobilized, well-characterized 'probe' molecules to capture complementary 'target' biomolecules suspended in a solution placed on the surface. The binding location of a target molecule allows it to be identified, typically using optical techniques. The success of this technology depends upon every target species in solution having the same opportunity to bind with its complementary probe spot, which may be anywhere on the surface. Achieving this probe–target interaction is not a trivial task: the established protocol for DNA screening covers the surface of a standard 7.5 cm × 2.5 cm glass slide with up to 30 000 different probe spots, and the need to minimize the target solution leads to very high-aspect-ratio fluid volumes that are typically only 25–50 μm deep. Conventional microarray analysis relies solely on diffusion of the target molecules to produce the necessary interactions, but these molecules are large and diffuse very slowly. Because of the relatively large surface area to be sampled, statistically significant results are achieved by using a large number of target molecules and running each test for a long time, typically 14–24 h. Both the sample size and the execution time limit the capabilities of this technology.

Mixing across the microarray surface by chaotic advection should improve this analysis technique in several ways.† Using fluid motion instead of diffusion for bulk molecule transport will produce results much more quickly. Maintaining a well-mixed solution will provide a homogeneous environment around each probe spot, reducing errors caused by spatial variations in the solution. Producing chaotic motion across the surface will enable each target molecule to eventually visit every probe spot on the microarray, which will increase the number of target molecules that bind to a

† An alternative approach is to abandon the traditional array slide and modify the geometry of the fluid domain (Cheek *et al.* 2001). However, we want to improve the technology without requiring significant changes in the supporting infrastructure.

probe spot and/or reduce the required number of target molecules. We wish, then, to address the following question: is it possible to draw from the existing chaotic advection literature and, with minimal additional analysis, establish a practical mixer design that significantly improves target–probe interactions in gene expression profiling applications? The answer, as outlined below, is 'yes'.

The first step in 'designing for chaos' is to identify the flows known to produce chaotic advection that can be implemented in our system. Fluid motion across the microarray surface can be modelled as Hele-Shaw flow. Under the Stokes flow approximation, the depth-averaged velocity is proportional to the gradient of the pressure (a scalar) and thus can be represented by a velocity potential. This correspondence between Hele-Shaw flow and potential flow, which has long been used to experimentally visualize pathlines in 2D ideal flow, allows us to consider existing analyses of chaotic advection in time-dependent, two-dimensional potential flows. As first noted by Evans *et al*. (1997), one obvious choice is the pulsed source–sink flow investigated by Jones & Aref (1988, hereafter denoted 'JA').

The original pulsed source–sink analysis in JA considers a single point source and a single point sink on the unbounded plane. The source and sink each have strength q and are operated alternately, with switching between the singularities occurring periodically at time-intervals of $T = A/q$, where A is the fluid area extracted (injected) during operation of the sink (source). An important component of this system is the procedure whereby fluid extracted at the sink is subsequently re-injected at the source. Any number of such re-injection procedures can be chosen; the analysis of JA concentrates primarily on a 'first out–first in' protocol that can be realized physically by collecting the extracted fluid in a tube beneath the sink, then turning the tube over and re-injecting the fluid at the source. This protocol assumes that the trajectory of a particle as it leaves the sink is a reflection about the vertical axis of its trajectory as it entered the source. Using standard dynamical systems tools such as Poincaré maps and Lyapunov exponents (see, for example, Lichtenberg & Lieberman 1992), JA show that the flow domain is dominated by chaotic advection over a wide range of operating parameters. The details of the chaos change with the re-injection procedure, but the occurrence of chaotic advection persists.

The nature of the results in JA is illustrated by the example shown in figure 1. The Poincaré map in figure 1*a* is generated by following the motion of a passive particle and recording its position in the plane after every cycle of duration $2T$. This Poincaré map shows the existence of regular regions, or *elliptic islands*, close to the source and sink, but much of the domain is occupied by the *chaotic sea*. A particle 'trapped' within an elliptic island follows a path that returns it to a point along the same closed curve in the Poincaré map after every operation cycle. The motion of such particles is not chaotic (stretching of material lines within an elliptic island is linear with iteration number instead of exponential) and thus the presence of these regular regions in the flow indicates a local resistance to mixing. The motion of a particle in the chaotic sea is characterized by periods of frequent extraction and re-injection interspersed with long forays away from the singularities along essentially curved paths. As shown in figure 1*b*, this behaviour can be quantified by examining the convergence of the maximum Lyapunov exponent, a quantity that gives the average exponential rate of divergence of two initially close particles. In the vicinity of the source and sink a fluid element in the chaotic sea experiences rapid stretching as a result of the frequent extraction and re-injection, but eventually this element is sent

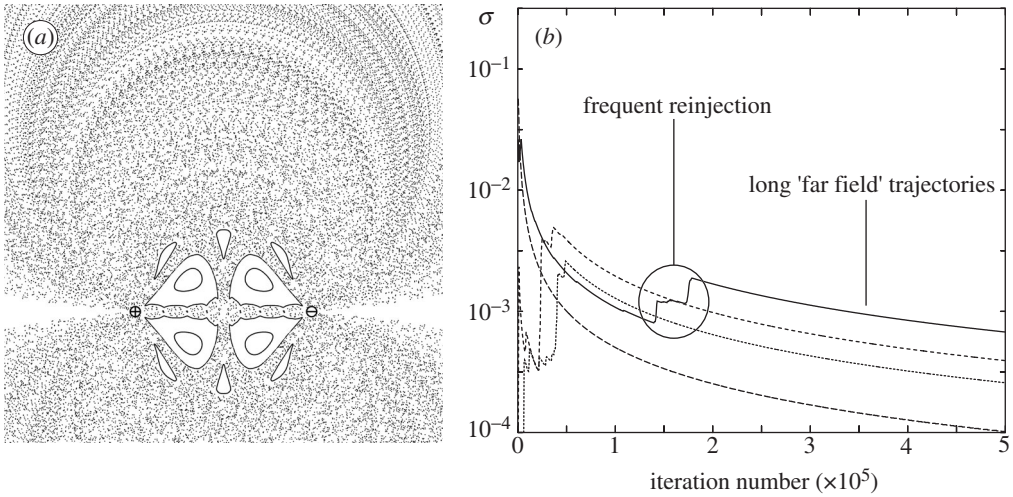

Figure 1. (*a*) Example Poincaré map for a pulsed source–sink system on the unbounded plane using the 'first out–first in' re-injection procedure. The source location is indicated by $\oplus$ and the sink by $\ominus$. The operating time T and strength q are chosen so that the sink (source) extracts (injects) a fluid area $A = \pi$. The sink is operated first in the cycle. This result can be compared directly with that in fig. 3*g* of JA. (*b*) Convergence of the maximum Lyapunov exponent σ for several chaotic trajectories in (*a*).

far from the source and sink on an essentially regular orbit. During this foray into the far-field the Lyapunov exponent attempts to converge to zero. With the recurrence of frequent extraction and re-injection, rapid stretching is again experienced.

As demonstrated by the existing analysis in JA, the re-injection process generates chaotic advection over much of the fluid domain, and the occurrence of chaos persists over a wide range of re-injection parameters and protocols, which suggests that efficient mixing can be achieved in a pulsed source–sink device without the need to precisely tune the system operation. The design could thus proceed from here without any further analysis being conducted, an approach that was taken by Evans *et al*. (1997) in proposing a micro-scale device for mixing two fluids. In the actual implementation, however, the flow domain will necessarily be bounded, which introduces changes to the system that presumably impact the extent and character of the chaos. The presence of a boundary also requires that the system now consist of source–sink *pairs*: there must be both a source and a sink operating at the same time in order to conserve the fluid volume in the chamber. Fortunately, analytic solutions exist for pulsed source–sink pairs in bounded 2D domains, and the analysis can be carried out similarly to that on the unbounded plane (M. A. Stremler 2004, unpublished research). It is thus fairly straightforward to verify that the occurrence of chaotic advection does indeed persist under these substantial changes.

The impact of these changes on the chaos can be evaluated in two steps by first considering the flow due to source–sink pairs on the unbounded plane and then considering the effect of a boundary. Since our objective is primarily to motivate the mixer design, we will examine the persistence of chaos for only a few cases. The discussion here will focus on the use of two source–sink pairs arranged on the vertices of a square.

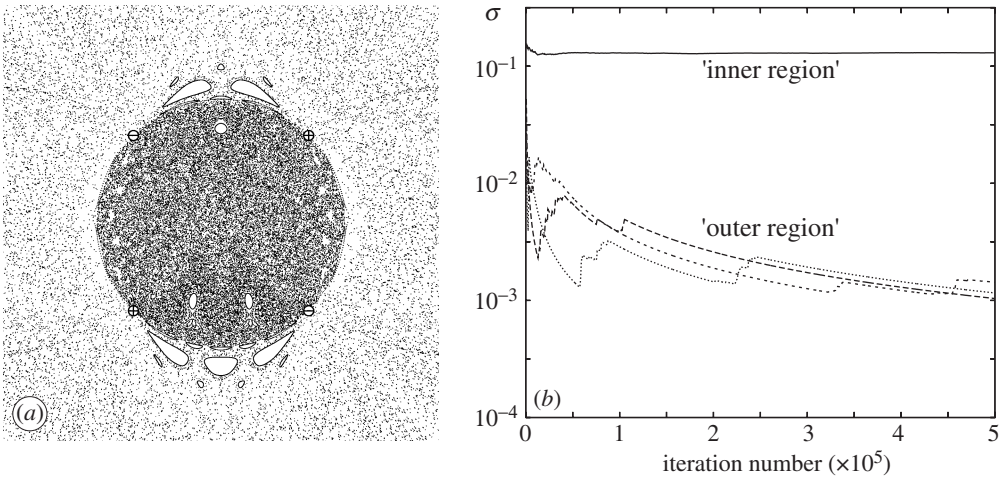

Figure 2. (*a*) Example Poincaré map for two source–sink pairs on the unbounded plane using the 'first out–first in' re-injection procedure. The sources (⊕) and sinks (⊖) are located at the vertices of a square with sides of length 2; paired sources and sinks are oriented on a vertical line. The operating time T and strength q for each pair are chosen so that the sink (source) extracts (injects) a fluid area $A = \pi$. The right-hand sink (and its paired source) are operated first in the cycle. (*b*) Convergence of the maximum Lyapunov exponent σ for several chaotic trajectories in (*a*). The 'inner region' is the central dark chaotic sea in (*a*), and the 'outer region' is the chaotic sea surrounding this 'inner region'.

The effects of introducing a second source and sink into the system are illustrated by comparing figures 1 and 2. When the distance between a 'non-paired' source and sink is much smaller than the distance between a paired source and sink, particle motions around the adjacent, 'non-paired' source and sink are the same as those found in the original unbounded plane analysis in figure 1. Placing the sources and sinks at the vertices of a square with sides of length 2 gives the results in figure 2. Bringing all sources and sinks close together has significant impact on the frequency with which some of the particles are re-injected. In fact, under the 'first out–first in' protocol used here, the central dark chaotic sea in the Poincaré map in figure 2*a* is generated by a single particle that never leaves this region of the plane. Thus, particles introduced near the singularities have an increased chance of avoiding the long, essentially regular trajectories that take it into the far field. Conversely, particles contained in the chaotic sea surrounding this 'inner region' stay outside and behave much like chaotic particles in figure 1*a*, with significant time spent traversing long paths in the far field. In general, using multiple source–sink pairs will increase re-injection frequency for some fraction of the particles regardless of pulse time or re-injection protocol.

The impact of frequent re-injection on mixing can be evaluated by examining the convergence of the Lyapunov exponents, as shown in figure 2*b*. Particles in the 'outer region', i.e. in the chaotic sea surrounding the central dark region in figure 2*a*, experience stretching rates similar to those in the system with just one source and one sink. In contrast, particles from the 'inner region' constantly experience frequent re-injection, which generates stretching rates that are two orders of magnitude greater than those for particles in the 'outer region'.

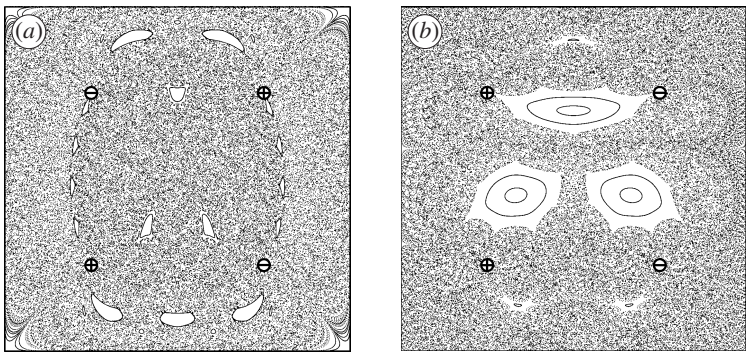

Figure 3. Poincaré maps for sources (⊕) and sinks (⊖) located at the vertices of a square with sides of length 2 in a square domain with sides of length 4. As in figure 1, the operating time T and strength q for each pair are chosen so that the sink (source) extracts (injects) fluid covering an area $A = \pi$. For both of these cases the right-hand sink (and its paired source) are operated first in the cycle. In (*a*), as in figure 2*a*, each source–sink pair lies on a vertical line, and the re-injection procedure is a 'first out–first in' protocol. Fluid extracted through the lower right sink is injected through the lower left source, and fluid extracted through the upper left sink is injected through the upper right source. In (*b*) each source–sink pair lies on a diagonal of the domain, and the re-injection procedure is a 'last out–first in' protocol. Fluid extracted through the lower right sink is injected through the lower left source, and fluid extracted through the upper right sink is injected through the upper left source.

Bounding the domain on a scale similar to the source–sink separations results in particle behaviours such as those illustrated in figure 3. The analytic solution assumes a slip condition at the domain boundary, so there is necessarily some lack of agreement between the model and the real flow in a thin region (of the order of the fluid depth) along the perimeter of the domain. Figure 3*a* uses the same source–sink configuration and re-injection protocol as in figure 2. Most of the elliptic islands present in figure 2*a* are still apparent, although their size, shape and location have changed slightly. The significant changes come about in the 'far-field' region, as particles are no longer allowed to move far from the singularities. The nearly regular curved paths are now restricted to the corners of the domain, and particles throughout most of the chaotic sea experience frequent re-injection similar to that of particles from the 'inner region' in figure 2*a*.

As expected, changing the source–sink configuration and the re-injection procedure affects the details of the chaotic advection. In figure 3*b* the paired sources and sinks lie on diagonals of the domain and the extracted fluid is re-injected according to a 'last out–first in' protocol. This re-injection method can be compared with collecting the extracted fluid in a tube beneath the sink, then sliding the tube to the source and re-injecting the fluid. The chaotic sea now clearly extends into the corners of the domain, but the three elliptic islands in the centre of the domain have grown significantly. However, while the details of the chaos have changed, the domain is still dominated by the chaotic sea.

These illustrative examples demonstrate that bounding the domain and adding source–sink pairs not only preserves the occurrence of chaos in the system but also should, in general, increase stretching rates and enhance mixing by forcing particles to be extracted and re-injected more frequently than in the unbounded domain

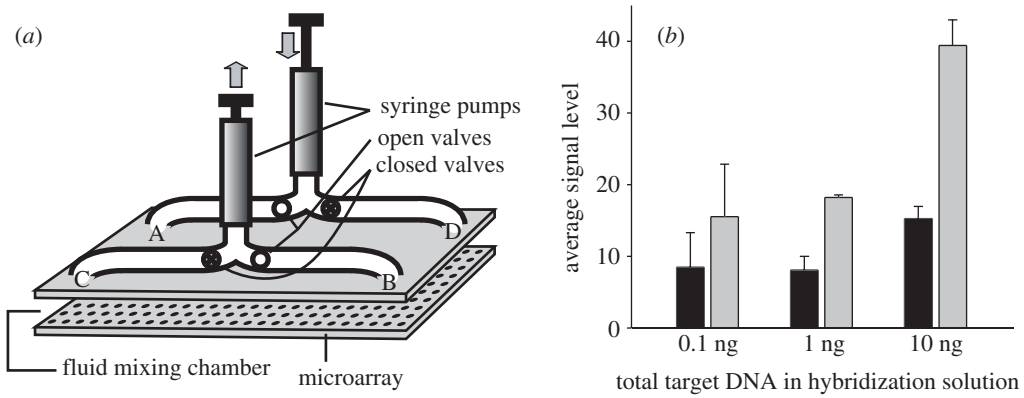

Figure 4. (*a*) Schematic of a pulsed source–sink chamber with external fluidic control. The fluid mixing chamber is *ca.* 5 cm × 2 cm × 25 µm and is sealed at the perimeter by a gasket (not shown). The configuration as shown has a source at A and a sink at B. Operating in this mode for time T generates the first half of a cycle. For the second half of a cycle, valve states switch, the syringe pumps reverse operation, and there is then a source at C and a sink at D. Fluid extracted from B is re-injected at C, and fluid extracted from D is re-injected at A. (*b*) Comparison of DNA hybridization results obtained with the standard diffusion-based method after 24 h (black bars) with hybridization results obtained with the pulsed source–sink chamber after 1 h (grey bars). Tests were run for three different target DNA concentrations. Error bars indicate target signal variability across an array of 102 identical probe spots. (Reproduced with permission from McQuain *et al.* (2004). Copyright (2004) Elsevier.)

with one source and one sink. We are thus able to proceed with confidence to our experimental design.

A schematic of the resulting pulsed source–sink chamber is shown in figure 4*a*. This design is very similar to that proposed by Evans *et al.* (1997). However, all pumping and valving is handled off-chip in a 'plug-and-play' approach that avoids many of the complications and expenses incurred with a fully self-contained lab-on-a-chip device (Tamanaha *et al.* 2002). This system is an implementation of the source–sink configuration and 'last out–first in' re-injection procedure used in figure 3*b*, although there is a delay between extraction and re-injection due to the physical distance between the paired source and sink. A real molecule is not likely to remember its extraction angle after having passed through the external plumbing; thus, in practice, large elliptic islands such as those in figure 3*b* will be destroyed.

The ability of this mixing chamber to enhance target–probe interactions in gene expression profiling applications is discussed in detail by McQuain *et al.* (2004). DNA targets are each tagged with fluorescent molecules, allowing their binding location to be detected optically. A solution of these labelled targets is placed on a microarray surface spotted with immobilized DNA probes. The signal level indicates the amount of tagged target DNA that is bonded to the surface by complementary probes. This signal is obtained by measuring the average pixel fluorescence intensity in the optical image of the surface. A summary of the experimental hybridization results is shown in figure 4*b* for a pulse volume that is approximately half of the domain volume. Experiments with mixing for 1 h with 0.1 ng of target DNA produced results that are statistically equivalent to those of a 24 h static hybridization using the same quantity

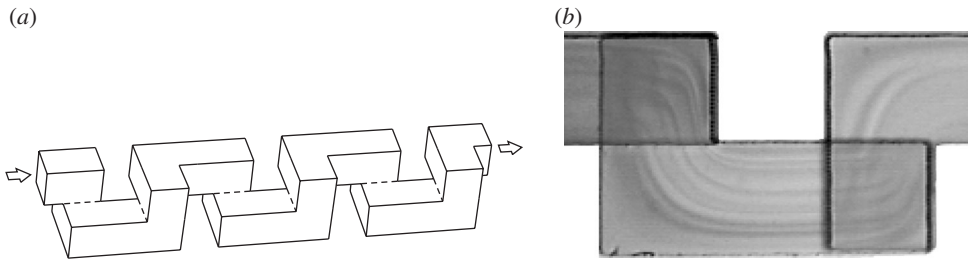

Figure 5. (*a*) Three segments of a 'serpentine' channel design. (*b*) Flow visualization of mixing in the 11th segment of the serpentine channel at $Re \approx 10$ as viewed from the top. Striations in the fluid caused by stretching and folding of the material interface are clearly visible. (Reproduced with permission from Beebe *et al*. (2001). Copyright (2001) Elsevier.)

of target (based on five runs). Experiments with mixing for 1 h with 1 ng and 10 ng of target DNA gave signal levels approximately 2.5 times greater than the comparable 24 h static hybridizations (based on three runs each). These experiments were all performed with identical spotted slides and the same batch of labelled targets. Thus, an increased signal indicates that more target molecules are bound to the surface. In addition to increased signal levels in shorter times, mixing was also found to give a threefold increase in signal-to-noise ratios and a twofold reduction in variation among replicate probe spots.

3. Passive mixing in a microchannel

Many 'lab-on-a-chip' systems require easily fabricated, integrated, 'flow-through' mixing of tiny fluid volumes, and a number of different microchannel designs have been presented in the literature for this purpose (see *parallel* and *serial lamination* in table 1). Several of these systems were designed using the principles of chaotic advection, although not all explicitly. For example, several of the serial lamination devices (e.g. Mensinger *et al*. 1994; Branebjerg *et al*. 1996; Gray *et al*. 1999) physically split and realign the fluid stream in a motion that mimics the baker's transformation (see, for example, Lichtenberg & Lieberman 1992).

One microchannel configuration that has been explicitly 'designed for chaos' is the serpentine channel shown schematically in figure 5*a* (Liu *et al*. 2000; Beebe *et al*. 2001; Vijayendran *et al*. 2003). This design is based on the observance by Jones *et al*. (1989, hereafter denoted 'JTA') of chaotic advection in a twisted pipe. The original analysis considered 180° arcs of circular pipe pieced together end to end. The system geometry was changed by varying the orientation angle χ between successive pipe segments. When $\chi = 0$ the pipe forms a torus, and when $\chi = 180°$ the pipe forms an S-shaped pattern with all segments in a plane. JTA found that for $\chi = 90°$ a significant cross-section of the pipe exhibits chaotic advection over a range of Reynolds numbers. This observation gave rise to the serpentine channel geometry shown in figure 4*a*, which can be viewed as a series of 90° 'arcs' placed end-to-end with an orientation angle of 90°.

The original twisted-pipe analysis of JTA assumed a small Dean number and no coupling of the fluid dynamics between successive pipe segments. Neither of these assumptions are valid for the geometry in figure 5*a*. Thus, in contrast to the analysis of the pulsed source–sink system, it is not clear *a priori* how much insight the ana-

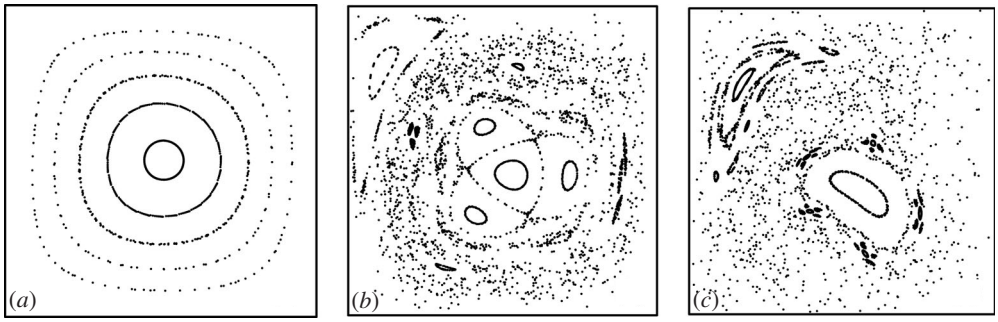

Figure 6. Poincaré maps for flow in the serpentine channel with Reynolds numbers of (*a*) 1, (*b*) 10 and (*c*) 20. Transition to chaos in the flow occurs for $1 < Re < 10$. (Reproduced with permission from Beebe *et al.* (2001). Copyright (2001) Elsevier.)

lytical model can lend to the analysis of chaotic advection in the serpentine channel, and so a computational approach has been taken. Chaotic advection was investigated by first computing the velocity field on a discrete grid using a commercially available computational fluid dynamics code (CFD-ACE+, CFD Research Corp., Huntsville, AL, USA). An infinite series of mixing segments was modelled by computing in a single segment with periodic velocity boundary conditions and a prescribed pressure drop across the segment. Particle traces were generated by numerical quadrature, with the velocity at any point in the channel determined as needed by interpolation of the discrete velocity field.

Poincaré maps for flow in the serpentine channel are shown in figure 6. For $Re = \mathcal{O}(1)$ the flow is predominantly regular and is thus not expected to mix well. For $Re \geqslant 10$, however, a significant portion of the channel cross-section exhibits chaotic advection and significant mixing enhancement should be observed.

A serpentine channel with a cross-section of 300 μm × 300 μm was fabricated in polydimethylsiloxane (PDMS) (Beebe *et al.* 2001). Two separate inlet streams join at a T-junction and then flow through 11 mixing segments; this implementation requires a device volume *ca.* 600 μm × 600 μm × 1.5 cm. Visualization of the mixing was accomplished by including phenolphthalein in one stream and an acid in the other. When the two colourless streams come in contact, the phenolphthalein turns red at the interface. As the two streams flow through the channel, this interface is stretched and folded by the chaos (for $Re \geqslant 10$), and diffusion across the interface accomplishes the desired mixing. Figure 5*b* shows an image of the 11th segment at $Re \approx 10$. Because of the small scale of the device, this image is obtained by integrating the intensity of phenol-red through the depth of the channel. The dark striations in figure 5*b* thus correspond to edge views of the acid–phenol interface as it winds back and forth through the channel cross-section. Comparison images were also taken in a single-layer 'zigzag' channel that does not produce chaotic advection. In this comparison case there is little stretching and folding of the material interface, and significantly less mixing was observed (Beebe *et al.* 2001).

The mixing enhancement achieved by this serpentine microchannel design has been used to improve the performance of a surface-based biosensor similar to the microarray example discussed in § 2 (Vijayendran *et al.* 2003).

4. Conclusions and outlook

Microfluidic devices that produce flows known to generate chaotic advection have proven to mix well, whether in essentially two-dimensional time-periodic flows or steady three-dimensional flows. Several mixers have now been based on this approach of 'designing for chaos', including those of Lee *et al.* (2001), Stroock *et al.* (2002), Niu & Lee (2003), Song *et al.* (2003) and Therriault *et al.* (2003) in addition to the two considered above. The capabilities of these devices should come as no surprise to the reader familiar with the history of chaotic advection. The phenomenon of chaotic advection does not hinge on any intrinsic scaling of the problem. Furthermore, the phenomenon appears quite robust to the change from model to actual flow. For example, the original investigation of chaotic advection considered a crude model of a stirred tank (Aref 1984) consisting of ideal flow induced by two fixed point vortices in a circular domain. Nevertheless, experimental evidence of mixing enhancement by chaotic advection in laminar flows that have only tenuous connection to the models has been readily achieved (e.g. Chien *et al.* 1986; Chaiken *et al.* 1986). The importance of laminar mixing in a number of emerging technologies has heightened awareness of this phenomenon, established a prominent platform for applications and provided impetus for developing a better understanding of chaos and mixing in laminar flows. It is quite likely that chaotic advection will continue to play an important role in applications of microfluidics for all the reasons we have stated.

A key element in the outlined process of 'designing for chaos' requires diagnosing and quantifying chaotic advection, and so a few comments on the available dynamical systems tools are appropriate. In this discussion we have relied exclusively on Poincaré maps and Lyapunov exponents; related tools include exit-time distributions and Kolmogorov entropy. Another set of important tools are based on invariant manifold theory (see, for example, Holmes 1984; Rom-Kedar *et al.* 1990; Beigie *et al.* 1994; MacKay 1994). This view is typically (but not necessarily) applied to small perturbations from an integrable system, in which case transport can be quantified using Melnikov-type methods (Balasuriya *et al.* 1998; Rom-Kedar & Poje 1999; Mezić 2001) or Kolmogorov–Arnold–Moser-type methods (Mezić & Wiggins 1994). Analysis based on perturbations of a known system, when applicable, can produce powerful results; a recent example is the experimental demonstration that global mixing can result when certain resonances are generated in a horizontal chain of vortices with Ekman pumping, even when the time dependence and three-dimensionality are weak (Solomon & Mezić 2003).

We remark that a very attractive approach to ensuring that chaotic advection will be present in a given flow device based on topological considerations of the stirred volume of fluid has recently been introduced (Boyland *et al.* 2000). This approach, although mathematically sophisticated, promises to make aspects of the design process quite intuitive. While this mathematical theory can guarantee the existence of a chaotically advected region, numerical experiments on the extent of that region are still required. Early calculations suggest that the chaotically advected region will be on the scale of the separation of the stirring elements (Finn *et al.* 2003).

The full potential of 'designing for chaos' on the microscale as presented in § 1 has yet to be realized. Device configurations have been based on systems known to generate chaotic advection, diagnostics have been computed to verify the occurrence

of chaos, and experimental verification of mixing enhancement has been observed. However, little study of optimization of device design has been performed.

It can, in fact, be said that the full potential of 'designing for chaos' has not yet been realized in any laminar mixing application. This is not to say that work has not been done to identify system parameters that maximize chaotic advection for a given flow; indeed, most investigations of chaotic advection include at least a partial parametric study. Examples that provide a fairly complete analysis include the identification of nearly globally chaotic 'mixing windows' in the partitioned pipe mixer (Ling 1993) and the identification of maximum entropy in time-dependent linear shear flow on a torus (D'Alessandro *et al*. 1999); see also the monograph by Ottino (1989). However, the step from maximizing chaos to optimizing mixing in practical applications has, in contrast, received very little consideration. One of the most complete investigations is the work by H. Brenner and co-workers (Bryden & Brenner 1996; Ganesan *et al*. 1997) on heat transfer in a rotating eccentric annular pipe, which they base in part on the chaotic advection analysis of Chaiken *et al*. (1986, 1987). The importance of performing this step from chaos to mixing is highlighted by their findings that, while chaotic advection has a substantial impact on heat transfer enhancement, optimal heat transfer does not correspond exactly to maximal chaos.

In summary, the technology of microfluidic devices provides significant motivation for considering laminar mixing and ways to optimize and enhance it. This topic is intimately connected to a deep analysis of the advection equations, viewed as a dynamical system, and a large body of analytical theory is available. Those systems known to generate chaotic advection provide a logical foundation from which to develop practical microscale mixers. The evidence suggests that there is great potential for achieving efficient mixing in devices that are 'designed for chaos'.

This work was made possible in part by the support of DARPA-MTO Grant #F33615-98-1-2853 and NIH Grant #1-R43-CA94601-01.

References

Adey, N. B. (and 13 others) 2002 Gains in sensitivity with a device that mixes microarray hybridization solution in a 25-μm-thick chamber. *Analyt. Chem.* **74**, 6413–6417.

Ajdari, A. 2001 Transverse electrokinetic and microfluidic effects in micropatterned channels: lubrication analysis for slab geometries. *Phys. Rev.* E **65**, 016301.

Anderson, R. C., Bogdan, G. J., Puski, A. & Su, X. 1998 Advances in integrated genetic analysis. In *Micro Total Analysis Systems 1998* (ed. D. J. Harrison & A. van den Berg), pp. 11–16. Dordrecht: Kluwer.

Anna, S. L., Bontoux, N. & Stone, H. A. 2003 Formation of dispersions using 'flow focusing' in microchannels. *Appl. Phys. Lett.* **82**, 364–366.

Aref, H. 1984 Stirring by chaotic advection. *J. Fluid Mech.* **143**, 1–21.

Aref, H. 1990 Chaotic advection of fluid particles. *Proc. R. Soc. Lond.* A **434**, 273–289.

Aref, H. 2002 The development of chaotic advection. *Phys. Fluids* **14**, 1315–1325.

Aref, H. & Balachandar, S. 1986 Chaotic advection in a Stokes flow. *Phys. Fluids* **29**, 3515–3521.

Arnol'd, V. I. 1965 Sur la topologie des écoulements stationnaires des fluides parfaits. *C. R. Hebd. Seanc. Acad. Sci. Paris* **261**, 17–20.

Ashwin, P. & King, G. P. 1995 Streamline topology in eccentric Taylor vortex flow. *J. Fluid Mech.* **285**, 215–247.

Balasuriya, S., Jones, C. K. R. T. & Sandstede, B. 1998 Viscous perturbations of vorticity: conserving flows and separatrix splitting. *Nonlinearity* **11**, 47–77.

Bau, H. H., Zhong, J. & Yi, M. 2001 A minute magnetohydrodynamic (MHD) mixer. *Sens. Actuat.* B **79**, 207–215.

Beebe, D. J., Adrian, R. J., Olsen, M. G., Stremler, M. A., Aref, H. & Jo, B.-H. 2001 Passive mixing in microchannels: fabrication and flow experiments. *Méc. Indust.* **2**, 343–348.

Beebe, D. J., Mensing, G. A. & Walker, G. M. 2002 Physics and applications of microfluidics in biology. *A. Rev. Biomed. Engng* **4**, 261–286.

Beigie, D., Leonard, A. & Wiggins, S. 1994 Invariant manifold templates for chaotic advection. *Chaos Solitons Fractals* **6**, 749–868.

Bertsch, A., Heimgartner, S., Causseau, P. & Renaud, P. 2001 Static micromixers based on large-scale industrial mixer geometry. *Lab Chip* **1**, 56–60.

Bertucci, F., Viens, P., Tagett, R., Nguyen, C., Houlgatte, R. & Birnbaum, D. 2003 DNA arrays in clinical oncology: promises and challenges. *Lab. Invest.* **83**, 305–316.

Bessoth, F. G., de Mello, A. J. & Manz, A. 1999 Microstructure for efficient continuous flow mixing. *Analyt. Commun.* **36**, 213–215.

Böhm, S., Greiner, K., Schlautmann, S., de Vries, S. & van den Berg, A. 2001 A rapid vortex micromixer for studying high-speed chemical reactions. In *Micro Total Analysis Systems 2001* (ed. J. M. Ramsey & A. van den Berg), pp. 25–27. Dordrecht: Kluwer.

Bökenkamp, D., Desai, A., Yang, X., Tai, Y.-C., Marzluff, E. M. & Mayo, S. L. 1999 Microfabricated silicon mixers for submillisecond quench-flow analysis. *Analyt. Chem.* **70**, 232–236.

Boyland, P. L., Aref, H. & Stremler, M. A. 2000 Topological fluid mechanics of stirring. *J. Fluid Mech.* **403**, 277–304.

Boyland, P. L., Stremler, M. A. & Aref, H. 2003 Topological fluid mechanics of point vortex motions. *Physica* D **175**, 69–95.

Branebjerg, J., Fabius, B. & Gravesen, P. 1994 Application of miniature analyzers: from microfluidic components to μTAS. In *Micro Total Analysis Systems 1994* (ed. A. van den Berg & P. Bergveld), pp. 141–151. Dordrecht: Kluwer.

Branebjerg, J., Gravesen, P., Krog, J. P. & Nielsen, C. R. 1996 Fast mixing by lamination. In *Proc. IEEE Int. Workshop Micro Electro Mechanical Systems, San Diego, CA, 11–15 February 1996*, pp. 441–446. New York: IEEE Press.

Bryden, M. D. & Brenner, H. 1996 Effect of laminar chaos on reaction and dispersion in eccentric annular flow. *J. Fluid Mech.* **325**, 219–237.

Chaiken, J., Chevray, R., Tabor, M. & Chan, Q. M. 1986 Experimental study of Lagrangian turbulence in a Stokes flow. *Proc. R. Soc. Lond.* A **408**, 165–174.

Chaiken, J., Chu, C. K., Tabor, M. & Tan, Q. M. 1987 Lagrangian turbulence and spatial complexity in Stokes flow. *Phys. Fluids* **30**, 687–694.

Cheek, B. J., Steel, A. B., Torres, M. P., Yu, Y. Y. & Yang, H. 2001 Chemiluminescence detection for hybridization assays on the flow-thru chip, a three-dimensional microchannel biochip. *Analyt. Chem.* **73**, 5777–5783.

Chien, W., Rising, H. & Ottino, J. M. 1986 Laminar mixing and chaotic mixing in several cavity flows. *J. Fluid Mech.* **170**, 355–377.

Choi, J.-W., Hong, C.-C. & Ahn, C. H. 2001 An electrokinetic active micromixer. In *Micro Total Analysis Systems 2001* (ed. J. M. Ramsey & A. van den Berg), pp. 621–622. Dordrecht: Kluwer.

Chován, T. & Guttman, A. 2002 Microfabricated devices in biotechnology and biochemical processing. *Trends Biotechnol.* **20**, 116–122.

Cunningham, D. D. 2001 Fluidics and sample handling in clinical chemical analysis. *Analysis Chim. Acta* **429**, 1–18.

D'Alessandro, D., Dahleh, M. & Mezić, I. 1999 Control of mixing in fluid flow: amaximum entropy approach. *IEEE Trans. Automatic Control* **44**, 1852–1863.

DeRisi, J. L. & Iyer, V. R. 1999 Genomics and array technology. *Curr. Opin. Oncol.* **11**, 76–79.

Deshmukh, A. A., Liepmann, D. & Pisano, A. P. 2000 Continuous micromixer with pulsatile micropumps. In *Technical Digest IEEE Solid State Sensors and Actuators Workshop, Hilton Head, SC, 4–8 June 2000*, pp. 73–76.

Ehrfeld, W., Golbig, K., Hessel, V., Löwe, H. & Richter, T. 1999 Characterization of mixing in micromixers by a test reaction: single mixing units and mixer arrays. *Ind. Engng Chem. Res.* **38**, 1075–1082.

Erbacher, C., Bessoth, F. G., Busch, M., Verpoorte, E. & Manz, A. 1999 Towards integrated continuous-flow chemical reactors. *Mikrochim. Acta* **131**, 19–24.

Evans, J., Liepmann, D. & Pisano, A. P. 1997 Planar laminar mixer. In *Proc. IEEE Int. Workshop Micro Electro Mechanical Systems, Nagoya, Japan, 26–30 January 1997*, pp. 96–101. New York: IEEE Press.

Evensen, H. T., Meldrum, D. R. & Cunningham, D. L. 1998 Automated fluid mixing in glass capillaries. *Rev. Scient. Instrum.* **69**, 519–526.

Finn, M. D., Cox, S. M. & Byrne, H. M. 2003 Topological chaos in inviscid and viscous mixers. *J. Fluid Mech.* **493**, 345–361.

Gad-el-Hak, M. (ed.) 2002 *The MEMS handbook*. Boca Raton, FL: CRC Press.

Ganesan, V., Bryden, M. D. & Brenner, H. 1997 Chaotic heat transfer enhancement in rotating eccentric annular-flow systems. *Phys. Fluids* **9**, 1296–1306.

Ghosh, S., Chang, H. C. & Sen, M. 1992 Heat transfer enhancement due to slender recirculation and chaotic transport between counter rotating eccentric cylinders. *J. Fluid Mech.* **238**, 119–154.

Glasgow, I. & Aubry, N. 2003 Enhancement of microfluidic mixing using time pulsing. *Lab Chip* **3**, 114–120.

Gobby, D., Angeli, P. & Gavriilidis, A. 2001 Mixing characteristics of T-type microfluidic mixers. *J. Micromech. Microengng* **11**, 126–132.

Gray, B. L., Jaeggi, D., Mourlas, N. J., van Drieënhuizen, B. P., Williams, K. R., Maluf, N. I. & Kovacs, G. T. A. 1999 Novel interconnection technologies for integrated microfluidic systems. *Sens. Actuat.* A **77**, 57–65.

Greiner, K. B., Deshpande, M., Gilbert, J. R., Ismagilov, R. F., Stroock, A. D. & Whitesides, G. M. 2000 Design analysis and 3D measurement of diffusive broadening in a Y-mixer. In *Micro Total Analysis Systems 2000* (ed. A. van den Berg, W. Olthius & P. Bergveld), pp. 87–90. Dordrecht: Kluwer.

Haverkamp, V., Ehrfeld, W., Gebauer, K., Hessel, V., Löwe, H., Richter, T. & Wille, C. 1999 The potential of micromixers for contacting of disperse liquid phases. *Fresenius J. Analyt. Chem.* **364**, 617–624.

He, B., Burke, B. J., Zhang, X., Zhang, R. & Regnier, F. E. 2001 A picoliter-volume mixer for microfluidic analytical systems. *Analyt. Chem.* **73**, 1942–1947.

Heller, M. J. 2002 DNA microarray technology: devices, systems, and applications. *A. Rev. Biomed. Engng* **4**, 129–153.

Hénon, M. 1966 Sur la topologie des lignes courant dans un cas particulier. *C. R. Hebd. Seances Acad. Sci. Paris* A **262**, 312–314.

Hinsmann, P., Frank, J., Svasek, P., Marasek, M. & Lendl, B. 2001 Design, simulation and application of a new micromixing device for time resolved infared spectroscopy of chemical reactions in solution. *Lab Chip* **1**, 16–21.

Holmes, P. J. 1984 Some remarks on chaotic particle paths in time-periodic, 3D swirling flows. In *Fluids and plasmas—geometry and dynamics* (ed. J. E. Marsden) Contemporary Mathematics, vol. 28, pp. 393-404. Providence, RI: American Mathematical Society.

Hong, C.-C., Choi, J.-W. & Ahn, C. H. 2001 A novel in-plane passive micromixer using Coanda effect. In *Micro Total Analysis Systems 2000* (ed. J. M. Ramsey & A. van den Berg), pp. 31–33. Dordrecht: Kluwer.

Horner, M., Metcalfe, G., Wiggins, S. & Ottino, J. M. 2002 Transport enhancement mechanisms in open cavities. *J. Fluid Mech.* **452**, 199–229.

Hosokawa, K., Fujii, T. & Endo, I. 2000 Formation and active mixing of metered nano/picoliter liquid droplets in a microfluidic device. In *Micro Total Analysis Systems 2000* (ed. A. van den Berg, W. Olthius & P. Bergveld), pp. 481–484. Dordrecht: Kluwer.

Jagannathan, H., Yaralioglu, G. G., Ergun, A. S. & Khuri–Yakub, B. T. 2003 An implementation of a microfluidic mixer and switch using micromachined acoustic transducers. In *Proc. IEEE Int. Conf. Micro Electro Mechanical Systems, Kyoto, Japan, 19–23 January 2003*, pp. 104–107. New York: IEEE Press.

Jones, S. W. & Aref, H. 1988 Chaotic advection in pulsed source–sink systems. *Phys. Fluids* **31**, 469–485.

Jones, S. W., Thomas, O. M. & Aref, H. 1989 Chaotic advection by laminar flow in a twisted pipe. *J. Fluid Mech.* **209**, 335–357.

Kakuta, M., Bessoth, F. & Manz, A. 2001 Microfabricated devices for fluid mixing and their application for chemical synthesis. *Chem. Record* **1**, 395–405.

Knight, J. B., Vishwanath, A., Brody, J. P. & Austin, R. H. 1998 Hydrodynamic focusing on a silicon chip: mixing nanoliters in microseconds. *Phys. Rev. Lett.* **80**, 3863–3866.

Koch, M., Chatelain, D., Evans, A. G. R. & Brunnschweiler, A. 1998 Two simple micromixers based on silicon. *J. Micromech. Microengng* **8**, 123–126.

Krasny, R. & Nitsche, M. 2002 The onset of chaos in vortex sheet flow. *J. Fluid Mech.* **454**, 47–69.

Kwon, O. & Zumbrunnen, D. A. 2001 Progressive morphology development to produce multilayer films and interpenetrating blends by chaotic mixing. *J. Appl. Polymer Sci.* **82**, 1569–1579.

Lee, Y.-K., Deval, J., Tabeling, P. & Ho, C.-M. 2001 Chaotic mixing in electrokinetically and pressure driven micro flows. In *Technical Digest IEEE Int. Conf. Micro Electro Mechanical Systems, Interlaken, Switzerland, 21–25 January 2001*, pp. 483–486.

Leong, C.-W. & Ottino, J. M. 1989 Experiments on mixing due to chaotic advection in a cavity. *J. Fluid Mech.* **209**, 463–499.

Lichtenberg, A. J. & Lieberman, M. A. 1992 *Regular and chaotic dynamics*, 2nd edn. Springer.

Ling, F. H. 1993 Chaotic mixing in a spatially periodic continuous mixer. *Phys. Fluids* A **5**, 2147–2160.

Liu, R. H., Stremler, M. A., Sharp, K. V., Olsen, M. G., Santiago, J. G., Adrian, R. J., Aref, H. & Beebe, D. J. 2000 Passive mixing in a three-dimensional serpentine microchannel. *J. MEMS* **9**, 190–197.

Liu, R. H., Yang, J., Pindera, M. Z., Athavale, M. & Grodzinski, P. 2002 Bubble-induced acoustic micromixing. *Lab Chip* **2**, 151–157.

Liu, R. H., Lenigk, R., Druyor-Sanchez, R. L., Yang, J. & Grodzinski, P. 2003 Hybridization enhancement using cavitation microstreaming. *Analyt. Chem.* **75**, 1911–1917.

Lu, L.-H., Ryu, K. S. & Liu, C. 2001 A novel microstirrer and arrays for microfluidic mixing. In *Micro Total Analysis Systems 2001* (ed. J. M. Ramsey & A. van den Berg), pp. 28–30. Dordrecht: Kluwer.

MacKay, R. S. 1994 Transport in 3D volume-preserving flows. *J. Nonlin. Sci.* **4**, 329–354.

McQuain, M. K., Seale, K., Peek, J., Fisher, T., Levy, S., Stremler, M. A. & Haselton, F. R. 2004 Chaotic mixer improves microarray hybridization. *Analyt. Biochem.* **325**, 215–226.

Meldrum, D. R. & Holl, M. R. 2002 Microscale bioanalytical systems. *Science* **297**, 1197–1198.

Meleshko, V. V. & Aref, H. 1996 A blinking rotlet model for chaotic advection. *Phys. Fluids* **8**, 3215–3217.

Mensinger, H., Richter, T., Hessel, V., Döpper, J. & Ehrfeld, W. 1994 Microreactor with integrated static mixer and analysis system. In *Micro Total Analysis Systems 1994* (ed. A. van den Berg & P. Bergveld), pp. 237–243. Dordrecht: Kluwer.

Mezić, I. 2001 Chaotic advection in bounded Navier–Stokes flows. *J. Fluid Mech.* **431**, 347–370.

Mezić, I. & Wiggins, S. 1994 On the integrability and perturbation of three-dimensional fluid flows with symmetry. *J. Nonlin. Sci.* **4**, 157–194.

Mitchell, M. C., Spikmans, V., Bessoth, F., Manz, A. & de Mello, A. 2000 Towards organic synthesis in microfluidic devices: multicomponent reactions for the construction of compound libraries. In *Micro Total Analysis Systems 2000* (ed. A. van den Berg, W. Olthius & P. Bergveld), pp. 463–465. Dordrecht: Kluwer.

Miyake, R., Lammerink, T. S. J., Elwenspoek, M. & Fluitman, J. H. J. 1993 Micro mixer with fast diffusion. In *Proc. Micro Electro Mechanical Systems, Fort Lauderdale, FL, 7–10 February 1993*, pp. 248–253. Piscataway, NJ: IEEE Press.

Mohr, S., Leikauf, G. D., Keith, G. & Rihn, B. H. 2002 Microarrays as cancer keys: an array of possibilities. *J. Clin. Oncol.* **20**, 3165–3175.

Mokrani, A., Castelain, C. & Peerhossaini, H. 1997 The effect of chaotic advection on heat transfer. *Int. J. Heat Mass Transf.* **40**, 3089–3104.

Moroney, R. M., White, R. M. & Howe, R. T. 1991 Microtransport induced by ultrasonic Lamb waves. *Appl. Phys. Lett.* **59**, 774–776.

Nguyen, N.-T. & Wereley, S. 2002 *Fundamentals and applications of microfluidics*. Boston, MA: Artech House.

Niu, X. & Lee, Y.-K. 2003 Efficient spatial-temporal chaotic mixing in microchannels. *J. Micromech. Microengng* **13**, 454–462.

Oddy, M. H., Santiago, J. G. & Mikkelsen, J. C. 2001 Electrokinetic instability micromixing. *Analyt. Chem.* **73**, 5822–5832.

Ottino, J. M. 1989 *The kinematics of mixing: stretching, chaos, and transport*. Cambridge University Press.

Pabit, S. A. & Hagen, S. J. 2002 Laminar-flow fluid mixer for fast fluorescence kinetics studies. *Biophys. J.* **83**, 2872–2878.

Pollack, L., Tate, M. W., Darnton, N. C., Knight, J. B., Gruner, S. M., Eaton, W. A. & Austin, R. H. 1999 Compactness of the denatured state of a fast-folding protein measured by submillisecond small-angle X-ray scattering. *Proc. Natl Acad. Sci. USA* **96**, 10 115–10 117.

Rife, J. C., Bell, M. I., Horwitz, J. S., Kabler, M. N., Auyeung, R. C. Y. & Kim, W. J. 2000 Miniature valveless ultrasonic pumps and mixers. *Sens. Actuat.* A **86**, 135–140.

Rom-Kedar, V. & Poje, A. C. 1999 Universal properties of chaotic transport in the presence of diffusion. *Phys. Fluids* **11**, 2044–2057.

Rom-Kedar, V., Leonard, A. & Wiggins, S. 1990 An analytical study of transport, mixing, and chaos in an unsteady vortical flow. *J. Fluid Mech.* **214**, 347–394.

Rothstein, D., Henry, E. & Gollub, J. P. 1999 Persistent patterns in transient chaotic fluid mixing. *Nature* **401**, 770–772.

Sato, K., Hibara, A., Tokeshi, M., Hisamoto, H. & Kitamori, T. 2003 Microchip-based chemical and biochemical analysis systems. *Adv. Drug. Deliv. Rev.* **55**, 379–391.

Schulte, T. H., Bardell, R. L. & Weigl, B. H. 2002 Microfluidic technologies in clinical diagnostics. *Clin. Chim. Acta* **321**, 1–10.

Schwesinger, N., Frank, T. & Wurmus, H. 1996 A modular microfluidic system with an integrated micromixer. *J. Micromech. Microengng* **6**, 99–102.

Sharp, K. V., Adrian, R. J., Santiago, J. G. & Molho, J. I. 2002 Liquid flows in microchannels. In *The MEMS handbook* (ed. M. Gad-el-Hak), vol. 6, pp. 1–38. Boca Raton, FL: CRC Press.

Solomon, T. H. & Mezić, I. 2003 Uniform resonant chaotic mixing in fluid flows. *Nature* **425**, 376–380.

Song, H., Tice, J. D. & Ismagilov, R. F. 2003 A microfluidic system for controlling reaction networks in time. *Angew. Chem. Int. Ed.* **42**, 767–772.

Stone, H. A. & Kim, S. 2001 Microfluidics: basic issues, applications, and challenges. *AIChE J.* **47**, 1250–1254.

Stroock, A. D., Dertinger, S. K. W., Ajdari, A., Mezić, I., Stone, H. A. & Whitesides, G. M. 2002 Chaotic mixer for microchannels. *Science* **295**, 647–651.

Tamanaha, C. R., Whitman, L. J. & Colton, R. J. 2002 Hybrid macro–micro fluidics system for a chip-based biosensor. *J. Micromech. Microengng* **12**, N7–N17.

Therriault, D., White, S. R. & Lewis, J. A. 2003 Chaotic mixing in three-dimensional microvascular networks fabricated by direct-write assembly. *Nature Mater.* **2**, 265–271.

Tuckerman, D. B. & Pease, R. F. W. 1981 High-performance heat sinking for VLSI. *IEEE Electron. Device Lett.* **2**, 126–129.

Vijayendran, R. A., Motsegood, K. M., Beebe, D. J. & Leckband, D. E. 2003 Evaluation of a three-dimensional micromixer in a surface-based biosensor. *Langmuir* **19**, 1824–1828.

Vivek, V., Zeng, Y. & Kim, E. S. 2000 Novel acoustic-wave micromixer. In *Proc. IEEE Int. Conf. Micro Electro Mechanical Systems, Miyazaci, Japan, 23–27 January 2000*, pp. 668–673. New York: IEEE Press.

Volpert, M., Mezić, I., Meinhart, C. D. & Dahleh, M. 1999 An actively controlled micromixer. In *Proc. ASME International Mechanical Engineering Congress, Nashville, TN, 14–19 November 1999*, pp. 483–487.

Wang, H., Iovenitti, P., Harvey, E. & Masood, S. 2002 Optimizing layout of obstacles for enhanced mixing in microchannels. *Smart Mater. Struct.* **11**, 662–667.

Weigl, B. H., Bardell, R. L. & Cabrera, C. R. 2003 Lab-on-a-chip for drug development. *Adv. Drug. Deliv. Rev.* **55**, 349–377.

Whitesides, G. M. & Stroock, A. D. 2001 Flexible methods for microfluidics. *Phys. Today* **54**, 42–48.

Woias, P., Hauser, K. & Yacoub-George, E. 2000 An active silicon micromixer for μTAS applications. In *Micro Total Analysis Systems 2000* (ed. A. van den Berg, W. Olthius & P. Bergveld), pp. 277–282. Dordrecht: Kluwer.

Xu, Y., Bessoth, F. G., Eijkel, J. C. T. & Manz, A. 2000 On-line monitoring of chromium (III) using a fast micromachined mixer/reactor and chemiluminescence detection. *Analyst* **125**, 677–683.

Yang, Z., Goto, H., Matsumoto, M. & Maeda, R. 2000 Active micromixer for microfluidic systems using lead-zirconate-titanate (PZT)-generated ultrasonic vibration. *Electrophoresis* **21**, 116–119.

Yang, Z., Matsumoto, S., Goto, H., Matsumoto, M. & Maeda, R. 2001 Ultrasonic micromixer for microfluidic systems. *Sens. Actuat.* A **93**, 266–272.

Yasuda, K. 2000 Non-destructive, non-contact handling method for biomaterials in microchamber by ultrasound. *Sens. Actuat.* B **64**, 128–135.

Yuen, P. K., Li, G., Bao, Y. & Müller, U. R. 2003 Microfluidic devices for fluidic circulation and mixing improve hybridization signal intensity on DNA arrays. *Lab Chip* **3**, 46–50.

Zhu, X. & Kim, E. S. 1998 Microfluidic motion generation with acoustic waves. *Sens. Actuat.* A **66**, 355–360.

Zumbrunnen, D. A. & Inamdar, S. 2001 Novel sub-micron highly multilayered polymer films formed by continuous flow chaotic mixing. *Chem. Engng Sci.* **56**, 3893–3897.